Properties of a chiral slab waveguide

John Lekner

Department of Physics, Victoria University of Wellington, Wellington, New Zealand

Received 12 January 1996, in final form 18 November 1996

Abstract. The symmetrized constitutive relations of Condon are used to find possible solutions in a waveguide formed from an isotropic chiral slab. Two eigenstates are found, related to positive and negative helicity plane-wave modes in an unbounded chiral medium. These eigenstates propagate along the slab, but are standing waves across the slab. Combinations of these eigenstates satisfy the boundary conditions when the slab is bounded by parallel conducting plates. The combinations are not transverse electric or transverse magnetic, but near cut-off these combinations correspond closely to TE or TM modes in achiral parallel-plate waveguides. Equations defining the dispersion relations are derived, and analytic solutions are obtained near cut-off and at high frequencies. At high frequencies one of the helicity eigenstates dominates, for all modes. Chirality of the slab medium splits the TE–TM degeneracy, but crossings of the dispersion curves are possible (and are demonstrated for a particular case).

A dielectric-clad waveguide is also considered. Analytic results are obtained for the low-frequency dispersion relations of the two fundamental modes. One of these modes approaches zero dispersion when the refractive index of the cladding tends to one of the indices of the two helicity eigenstates in the slab.

1. Introduction

The propagation of electromagnetic waves in waveguides filled with a chiral (optically active) medium has been examined in the papers [1–14]. Of these publications, [1, 7, 11] deal with a chiro-waveguide formed by parallel conducting plates. We re-examine this problem and explore the properties of the propagating modes and of their dispersion relations. We obtain analytic expressions for the wavevector K near the cut-off $K = 0$ (which occurs at different frequencies for different modes), and also at high frequency. We find that near cut-off the modes have predominantly transverse magnetic (TM) or transverse electric (TE) character. We verify Mahmoud's [7] assumption that the electric fields of the modes are either even or odd when expressed in terms of a coordinate centred midway between the conducting plates, and also his numerical deduction that one helicity always dominates at high frequency. (Which one dominates depends on the sign of the chirality.) We also find that crossings of the dispersion relations (wavevector versus frequency curves) are possible for modes of different symmetry, and discuss when these can occur.

Although the assumption of ideal conducting plates is adequate at microwave frequencies, the attenuation at optical frequencies would be considerable. Section 6 explores the properties of a chiral slab clad with dielectric. Analytic results are obtained for the dispersion relation at low frequency. We show that the fundamental modes bifurcate at zero frequency. When the chiral index is small compared to the difference in the slab and cladding refractive indices, the modes are TE and TM in character. Index matching

0963-9659/97/030373+12$19.50

enhances the effect of chirality, and one mode disappears when the chirality index is equal to the difference in slab and cladding indices.

As our basis electromagnetic relations we use the two curl equations

$$c\nabla\times\boldsymbol{E} = -\partial\boldsymbol{B}/\partial t \qquad c\nabla\times\boldsymbol{H} = \partial\boldsymbol{D}/\partial t \tag{1}$$

and the symmetrized Condon [15] gyrotropic constitutive relations

$$\boldsymbol{D} = \epsilon\boldsymbol{E} - g\partial\boldsymbol{H}/\partial t \qquad \boldsymbol{B} = \mu\boldsymbol{H} + g\partial\boldsymbol{E}/\partial t \tag{2}$$

which have been selected by Silverman [16] as the most likely to be the correct choice among the ones in use. The equations are linear, so we can deal with one Fourier component at a time; we assume a time dependence $e^{-i\omega t}$, and set $\omega g = \gamma$, the chirality index. (The index of refraction of the two modes of positive and negative helicity is $n+\gamma$ and $n-\gamma$, where $n = \sqrt{\epsilon\mu}$ [16, 17].) The equations (1) and (2) simplify to

$$c\nabla\times\boldsymbol{E} = i\omega\boldsymbol{B} \qquad c\nabla\times\boldsymbol{H} = -i\omega\boldsymbol{D} \tag{3}$$

$$\boldsymbol{D} = \epsilon\boldsymbol{E} + i\gamma\boldsymbol{H} \qquad \boldsymbol{B} = \mu\boldsymbol{H} - i\gamma\boldsymbol{E}\,. \tag{4}$$

The result of eliminating $\boldsymbol{B}, \boldsymbol{H}$ and $\boldsymbol{D}$ is [17]

$$\mu\nabla\times\left(\frac{1}{\mu}\nabla\times\boldsymbol{E}\right) = \left(\epsilon\mu-\gamma^2\right)\frac{\omega^2}{c^2}\boldsymbol{E} + \frac{\omega}{c}\left[\gamma\nabla\times\boldsymbol{E} + \mu\nabla\times\left(\frac{\gamma}{\mu}\boldsymbol{E}\right)\right]. \tag{5}$$

The equation for $\boldsymbol{H}$ is similar, with ϵ and μ changing roles:

$$\epsilon\nabla\times\left(\frac{1}{\epsilon}\nabla\times\boldsymbol{H}\right) = \left(\epsilon\mu-\gamma^2\right)\frac{\omega^2}{c^2}\boldsymbol{H} + \frac{\omega}{c}\left[\gamma\nabla\times\boldsymbol{H} + \epsilon\nabla\times\left(\frac{\gamma}{\epsilon}\boldsymbol{H}\right)\right]. \tag{6}$$

2. Propagation in a homogeneous chiral slab

The above equations hold for an arbitrary inhomogeneous medium. We now assume ϵ, μ and γ are constant within the slab, that the wavefront propagates in the x direction and that the field components are independent of y. Then all fields carry the factor $e^{i(Kx-\omega t)}$; apart from this factor, the spatial dependence is on z only. Let primes denote differentiation with respect to z, and let

$$k_\gamma^2 = \left(\epsilon\mu-\gamma^2\right)\omega^2/c^2 = k_+k_- \tag{7}$$

where $k_\pm = n_\pm\omega/c = (n\pm\gamma)\omega/c$, with $n = (\epsilon\mu)^{1/2}$. Then the coupled equations (5) for the components of $\boldsymbol{E}$ reduce to

$$\begin{aligned}
&E_x'' + k_\gamma^2 E_x - 2\gamma\frac{\omega}{c}E_y' - iKE_z' = 0\\
&2\gamma\frac{\omega}{c}E_x' + E_y'' + \left(k_\gamma^2 - K^2\right)E_y - 2i\gamma\frac{\omega}{c}KE_z = 0\\
&-iKE_x' + 2i\gamma\frac{\omega}{c}KE_y + \left(k_\gamma^2 - K^2\right)E_z = 0\,.
\end{aligned} \tag{8}$$

These differential equations have constant coefficients, and thus have sinusoidal solutions. We seek standing wave solutions, and note that in each equation E_y and E_z always differ by one derivative from E_x. Thus a standing wave solution has to be of the form (we omit the $e^{-i\omega t}$ time dependence)

$$\boldsymbol{E} = \left[X\sin(qz+\phi),\, Y\cos(qz+\phi),\, Z\cos(qz+\phi)\right]e^{iKx}\,. \tag{9}$$

Substitution of (9) into the set (8) gives three equations linear and homogeneous in X, Y and Z. A non-zero solution exists only if the determinant of coefficients is zero:

$$\begin{vmatrix} k_\gamma^2 - q^2 & 2\gamma\dfrac{\omega}{c}q & \mathrm{i}Kq \\ 2\gamma\dfrac{\omega}{c}q & k_\gamma^2 - q^2 - K^2 & -2\mathrm{i}\gamma\dfrac{\omega}{c}K \\ -\mathrm{i}Kq & 2\mathrm{i}\gamma\dfrac{\omega}{c}K & k_\gamma^2 - K^2 \end{vmatrix} = 0\,. \tag{10}$$

This reduces to a quadratic equation for $K^2 + q^2$, with solutions

$$\left(K^2 + q^2\right)_\pm \equiv k_\pm^2 = \left(\sqrt{\epsilon\mu} \pm \gamma\right)^2 \omega^2/c^2\,. \tag{11}$$

Thus, just as in an unbounded chiral medium, there are two effective wavenumbers $k_\pm = n_\pm\omega/c$ in the slab, with corresponding indices

$$n_\pm = \sqrt{\epsilon\mu} \pm \gamma \equiv n \pm \gamma\,. \tag{12}$$

The associated electric field eigenvectors are given by (9), with $[X, Y, Z]$ proportional to

$$[q_+, k_+, \mathrm{i}K_+] \qquad \text{or} \qquad [q_-, -k_-, \mathrm{i}K_-]\,. \tag{13}$$

3. Dispersion relations for a chiral slab between conducting plates

We take the conducting plates to be at $z = 0$ and $z = d$, and assume zero $\boldsymbol{E}$ and $\boldsymbol{B}$ inside the plates (ideal conductors). The boundary conditions are that the parallel components (E_x and E_y) of $\boldsymbol{E}$ and the normal component (B_z) of $\boldsymbol{B}$ are zero at the plates.

The solutions (9), (13) do not permit these boundary conditions to be satisfied for either of the pure positive or negative helicity eigenstates. The boundary conditions can be satisfied by a mix of eigenstates if q_+ and q_- are such that K_+ and K_- take a common value:

$$k_+^2 - q_+^2 = K^2 = k_-^2 - q_-^2\,. \tag{14}$$

Then combining the two helicity eigenstates with amplitudes 1 and A gives an electric field with components

$$\left[q_+s_+ + Aq_-s_-, k_+c_+ - Ak_-c_-, \mathrm{i}K(c_+ + Ac_-)\right]\mathrm{e}^{\mathrm{i}Kx} \tag{15}$$

where $s_\pm = \sin(q_\pm z + \phi_\pm)$, $c_\pm = \cos(q_\pm z + \phi_\pm)$. The conditions $E_x = 0$ and $E_y = 0$ at $z = 0$ and $z = d$ are satisfied if

$$\begin{aligned} &q_+ \sin\phi_+ + Aq_- \sin\phi_- = 0 \qquad && k_+ \cos\phi_+ - Ak_- \cos\phi_- = 0 \\ &q_+ \sin\chi_+ + Aq_- \sin\chi_- = 0 \qquad && k_+ \cos\chi_+ - Ak_- \cos\chi_- = 0 \end{aligned} \tag{16}$$

where $\chi_\pm = q_\pm d + \phi_\pm$. ($B_z$ is proportional to E_y from equation (3) for the curl of $\boldsymbol{E}$, and will be zero at the boundaries if E_y is zero there.) Thus

$$A = -\frac{q_+ \sin\phi_+}{q_- \sin\phi_-} = \frac{k_+ \cos\phi_+}{k_- \cos\phi_-} = -\frac{q_+ \sin\chi_+}{q_- \sin\chi_-} = \frac{k_+ \cos\chi_+}{k_- \cos\chi_-}\,. \tag{17}$$

It follows that the dispersion relations (expressing K as a function of k) are contained in

$$\frac{q_+}{k_+}\tan\phi_+ + \frac{q_-}{k_-}\tan\phi_- = 0 \tag{18}$$

$$\frac{q_+}{k_+}\tan\chi_+ + \frac{q_-}{k_-}\tan\chi_- = 0\,. \tag{19}$$

In the achiral limit there are TM and TE modes:

$$\text{TM:}\quad \phi_\pm \to 0, \quad A \to 1, \quad \boldsymbol{E} \sim [q \sin qz, 0, \mathrm{i}K \cos qz]\mathrm{e}^{\mathrm{i}Kx} \tag{20}$$

$$\text{TE:}\quad \phi_\pm \to \pi/2, \quad A \to -1, \quad \boldsymbol{E} \sim [0, \sin qz, 0]\mathrm{e}^{\mathrm{i}Kx}\,. \tag{21}$$

In both cases $qd = m\pi$ with m an integer ($m = 0$ is possible only for the TM case, which then becomes a TEM mode), so the achiral wavenumber is obtained from $k = n\omega/c$ by

$$K = (k^2 - q^2)^{1/2} = [k^2 - (m\pi/d)^2]^{1/2}\,. \tag{22}$$

The TM and TE modes are degenerate for $m \geqslant 1$ in the achiral limit: figure 1 shows the dispersion relations, which in this case are straight lines of unit slope in the K^2 versus k^2 diagram, originating at the points $k = m\pi/d$, $K = 0$. We expect chirality to remove the degeneracy, in which modes with different fields have the same dispersion relation, except for the nondegenerate TEM mode.

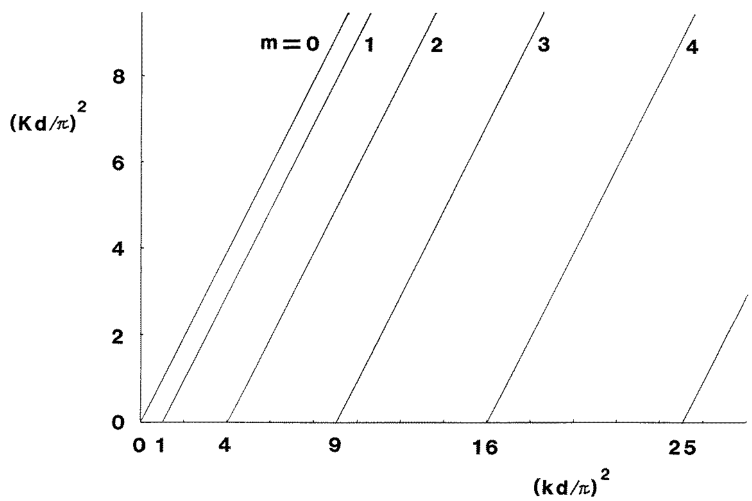

Figure 1. Dispersion relations for propagating modes in a parallel-plate waveguide filled with an achiral medium. The wavevector is K, the angular frequency is ck/n, where n is the refractive index of the slab. The spacing between the conducting plates is d, and we plot $(Kd/\pi)^2$ versus $(kd/\pi)^2 = (2d/\lambda)^2$. The straight lines originate at $kd = m\pi$, and for $m > 0$ represent both TM and TE modes.

The equations (17) are satisfied by

$$\chi_\pm = (\ell\pi + q_\pm d)/2 \qquad \phi_\pm = (\ell\pi - q_\pm d)/2 \tag{23}$$

for zero or integer ℓ, provided

$$\frac{q_+}{k_+}\tan(\ell\pi/2 \pm q_+ d/2) + \frac{q_-}{k_-}\tan(\ell\pi/2 \pm q_- d/2) = 0\,. \tag{24}$$

For zero or even ℓ the dispersion relation is determined by

$$\frac{q_+}{k_+}\tan(q_+ d/2) + \frac{q_-}{k_-}\tan(q_- d/2) = 0 \tag{25}$$

and the mixing ratio is

$$A_{\tan} = \frac{k_+ \cos(q_+ d/2)}{k_- \cos(q_- d/2)} = -\frac{q_+ \sin(q_+ d/2)}{q_- \sin(q_- d/2)}\,. \tag{26}$$

For even ℓ we have $c_\pm = \cos(q_\pm\zeta)\cos(\ell\pi/2)$ and $s_\pm = \sin(q_\pm\zeta)\cos(\ell\pi/2)$ where $\zeta = z - d/z$. Thus the transverse components of the electric field (E_y and E_z) are even in ζ, the displacement from the plane midway between the conducting plates bounding the chiral slab.

For odd ℓ the relation between K and k (i.e. between the propagation wavevector and the frequency) is found from

$$\frac{q_+}{k_+}\cot(q_+d/2) + \frac{q_-}{k_-}\cot(q_-d/2) = 0\,. \tag{27}$$

For odd ℓ we have $c_\pm = -\sin(q_\pm\zeta)\sin(\ell\pi/2), s_\pm = \cos(q_\pm\zeta)\sin(\ell\pi/2)$, and so the transverse components of the electric field are odd in ζ. Thus the modes may be classified into even and odd, as was assumed by Mahmoud [7]. The mixing ratio for odd ℓ is

$$A_{\mathrm{cot}} = \frac{k_+\sin(q_+d/2)}{k_-\sin(q_-d/2)} = -\frac{q_+\cos(q_+d/2)}{q_-\cos(q_-d/2)}\,. \tag{28}$$

4. Properties of the dispersion relations

In the chiral slab at the cut-off $K = 0$ we have $q_+ = k_+$ and $q_- = k_-$. The conditions (18) and (19) then imply $\tan(k_+d) + \tan(k_-d) = 0$, which is solved by $kd = m\pi$, since $k_\pm = k(1 \pm \gamma/n)$. Thus all modes made up from the two chiral eigenstates have dispersion relations which start at $K = 0$ with the zero-chirality values $k = m\pi/d$.

We first examine the 'TEM' mode, the chiral analogue of the $m = 0$ TM case which has $K = k$. It is clear that (25) cannot be satisfied if both q_+ and q_- are real and less than π/d. We write G for γ/n; then $k_\pm = k(1 \pm G)$ and

$$q_\pm^2 = k^2 - K^2 + (\pm 2G + G^2)k^2\,. \tag{29}$$

We take (for the moment) the chiral index γ to be positive. Then q_+ will be real and $q_- = \mathrm{i}|q_-|$ will be imaginary, with

$$q_-^2 = (1+G)^2k^2 - K^2 \qquad |q_-|^2 = K^2 - (1-G)^2k^2 \tag{30}$$

and

$$q_+^2 + |q_-|^2 = 4k^2G\,. \tag{31}$$

Equation (25) now reads

$$\frac{q_+}{k_+}\tan(q_+d/2) = \frac{|q_-|\tanh(|q_-|d/2)}{k_-}\,. \tag{32}$$

At small kd this has the solution

$$K^2 = k^2\left\{1 - G^2\left[1 - (kd)^2(1-G^2)/3\right]\right\} + \mathrm{O}\left\{G^4(kd)^6\right\} \tag{33}$$

and q_+ and $|q_-|$ are both equal to $k(2G)^{1/2}$ to lowest order in G.

At large kd we see from (32) that q_+d must tend to π from below; we set $q_+d = \pi - \delta$ in (31) and (32) and solve for δ:

$$\delta = \pi\frac{1-G}{1+G}\big(kd\sqrt{G}\big)^{-1} + \mathrm{O}\big(kd\sqrt{G}\big)^{-2}\,. \tag{34}$$

Thus the asymptotic behaviour of the dispersion relation is

$$K^2 = k_+^2 - \frac{\pi^2}{d^2}\left\{1 - \frac{1-G}{1+G}\frac{2}{kd\sqrt{G}}\right\} + \mathrm{O}(kd\sqrt{G})^{-2}\,. \tag{35}$$

This relation is in agreement with the numerical finding of Mahmoud [7] that, when the chirality index is positive, the high-frequency limit of each mode has the propagation wavevector approaching k_+.

As $k \to 0$ we find from (30), (33) and (26) that

$$q_+^2 \to 2G(1+G)k^2 \qquad |q_-|^2 \to 2G(1-G)k^2 \qquad A \to \frac{1+G}{1-G}\,. \tag{36}$$

Thus the ratio of negative to positive helicity in the $m = 0$ mode tends to unity as the chirality index tends to zero, which justifies the label 'TEM' for this mode. At large kd we have, using (36),

$$q_+ \to \pi/d \qquad |q_-| \to 2k\sqrt{G} \qquad A \to 0\,. \tag{37}$$

Thus the positive helicity eigenstate dominates in this mode at high frequency, in accord with the result $K \to k_+$ deduced from (35).

We now look at the modes that start in pairs at $kd = m\pi$, with $m \geqslant 1$. In the achiral limit these occur in degenerate pairs, the TM_m and TE_m modes, with negative to positive helicity field ratios $A = 1$ and $A = -1$, respectively. For the achiral modes starting at $kd = m\pi$, $K^2 = k^2 - (m\pi/d)^2$, so that qd is fixed at $m\pi$. For the chiral slab we find from equations (25) and (27) that near $kd = m\pi$,

$$K^2 = \left[k^2 - (m\pi/d)^2\right]\frac{(1-G^2)^2}{1-G^2 \pm (-)^m 2G\sin(m\pi G)/m\pi} + \mathrm{O}\left[k^2 - (m\pi/d)^2\right]^2 \tag{38}$$

where the minus sign applies to the tangent relation (25) and the plus sign to the cotangent relation (27). Thus the transverse wavenumbers $q_\pm$, defined by $q_\pm^2 = k_\pm^2 - K^2$, are

$$q_\pm = (1 \pm G)m\pi/d + \mathrm{O}\left[k^2 - (m\pi/d)^2\right]. \tag{39}$$

From this result and equations (26) and (28) we find that at $k = m\pi/d$ the modes satisfying the tangent relation (25) have mixing ratio

$$A_{\tan} \to \frac{1+G}{1-G}\,\frac{\cos[(1+G)m\pi/2]}{\cos[(1-G)m\pi/2]} = \frac{1+G}{1-G}(-)^m \tag{40}$$

while those satisfying the cotangent relation (27) have ratio of negative to positive helicity amplitudes

$$A_{\cot} \to -\frac{1+G}{1-G}\,\frac{\cos[(1+G)m\pi/2]}{\cos[(1-G)m\pi/2]} = -\frac{1+G}{1-G}(-)^m\,. \tag{41}$$

Thus for even m the ℓ = even (tangent) modes are 'TM', and the ℓ = odd (cotangent) modes are 'TE', near $k = m\pi/d$. For odd m the assignments of 'TM' and 'TE' characteristics are reversed.

At large kd the $m > 0$ modes become predominantly of positive helicity character, if the chirality index $\gamma = Gn$ is positive. We look at the tangent relation (25) first. At $kd = m\pi$, $q_\pm d = (1 \pm G)m\pi$ (both real for $m > 0$); as kd increases we expect $q_+ d/2$ to tend to an odd multiple of $\pi/2$ from below, and q_- to become imaginary. We set $q_+ d = (2M+1)\pi - \delta$ in (25) and solve for the small quantity δ to find

$$q_+ d \to (2M+1)\pi\left\{1 - \frac{1-G}{1+G}\left(kd\sqrt{G}\right)^{-1}\right\}. \tag{42}$$

Thus q_+^2 tends to a constant and $K^2 = k_+^2 - q_+^2$ differs from k_+^2 by a constant, in the limit of large kd. In the same limit, $q_-^2 = k_-^2 - K^2 = q_+^2 - (k_+^2 - k_-^2) = q_+^2 - 4k^2 G$ decreases linearly with k^2, with slope $-4G$.

In the case of the cotangent relation (27) we set $q_+d = 2N\pi - \delta$, since we need $q_+d/2$ to approach a multiple of π from below. We find

$$q_+d \to 2N\pi \left\{1 - \frac{1-G}{1+G}\left(kd\sqrt{G}\right)^{-1}\right\} \tag{43}$$

and again q_-^2 becomes negative and decreases linearly with k^2 for large kd. In both the even (tangent) and odd (cotangent) modes the positive helicity character dominates when $G > 0$.

5. Mode cross-over

Figure 2 shows the variation of the square of the wavevector K versus the square of the frequency. (We actually plot the dimensionless quantity $(Kd/\pi)^2$ versus $(kd/\pi)^2$; note that $k = n\omega/c = n2\pi/\lambda$, so $kd/\pi = 2nd/\lambda$, where λ is the vacuum wavelength.) We see that the behaviour of the wavevector is in accord with the discussion of the previous section; in addition we note two crossings of the dispersion relations for even and odd modes of the same m. Thus it is possible for the two modes of different symmetry to have the same phase speed ω_c/K at a given angular frequency ω_c. This can happen when q_+d and q_-d are both integer multiples of π:

$$q_+d = P\pi \qquad \text{and} \qquad q_-d = N\pi \tag{44}$$

with P and N both even, or both odd. We then have

$$k_+^2 - K^2 = (P\pi/d)^2 \qquad \text{and} \qquad k_-^2 - K^2 = (N\pi/d)^2 \tag{45}$$

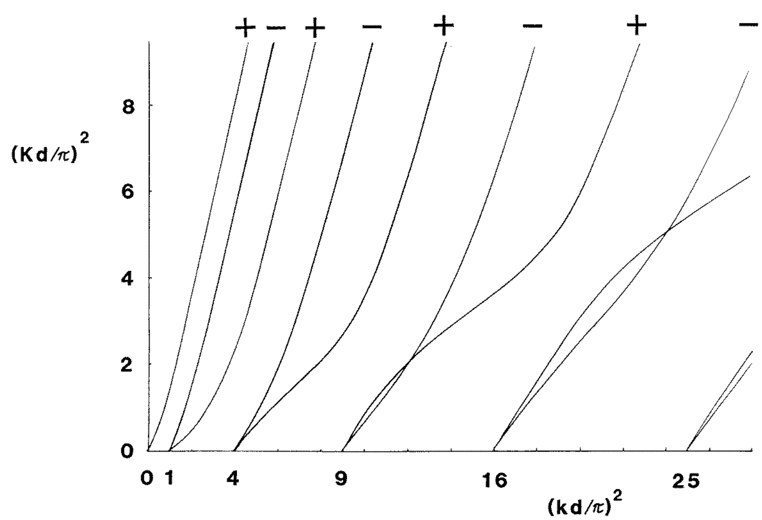

Figure 2. Dispersion relations for a waveguide formed from a chiral slab between conducting plates. The refractive indices of positive and negative helicity eigenstates are $n(1 \pm G)$. The $(Kd/\pi)^2$ versus $(kd/\pi)^2$ curves are plotted for $G = \frac{1}{2}$. Modes with even transverse electric fields have dispersion curves determined by the tangent relation (25) and are denoted by '+'. Modes with odd transverse electric fields satisfy the cotangent relation (27) and are denoted by '−'. Note that K^2 tends to k_+^2 minus a constant for large Kd (when $G > 0$).

and since $k_\pm = (1 \pm G)k$, the difference of the left-hand sides of (45) gives $k_+^2 - k_-^2 = 4Gk^2$, so that cross-overs can occur when

$$\left(\frac{kd}{\pi}\right)^2 = \frac{P^2 - N^2}{4G} \tag{46}$$

where P and N are integers. The two cross-overs in figure 2, which is drawn for $G = \frac{1}{2}$, occur at $(P, N) = (5, 1)$ and $(7, 1)$.

6. Chiral slab with dielectric cladding

Dissipation of energy in the bounding metal plates at optical frequencies will be high, so we will now examine the case of a chiral slab with dielectric cladding. As above, we will characterize the chiral medium by the constants ϵ, μ and γ, and we will assume the bounding dielectric to be thick compared to the wavelength and be characterized by ϵ_1 and μ_1, and $n = (\epsilon_1\mu_1)^{1/2}$. The thickness of the chiral slab is d as before.

The previous analysis showed that the possible propagating modes within the chiral slab have y and z components of the electric field which are even or odd in the displacement from the mid-plane of the slab. We take the dielectric cladding to occupy $|z| \geqslant d/2$, and look for exponentially decreasing (evanescent) electric field solutions of the form

$$\boldsymbol{E}_1 = [X_1, Y_1, Z_1] \exp\left[\mathrm{i}Kx - |q_1|(z - d/2)\right] \tag{47}$$

for $z \geqslant d/2$. From equations (8) with $\gamma = 0$ we have, with $k_1 = n_1\omega/c$,

$$\begin{aligned} &(|q_1|^2 + k_1^2)X_1 + \mathrm{i}K|q_1|Z_1 = 0 \\ &(|q_1|^2 + k_1^2 - K^2)Y_1 = 0 \\ &\mathrm{i}K|q_1|X_1 + (k_1^2 - K^2)Z_1 = 0\,. \end{aligned} \tag{48}$$

The determinant of the coefficients of X_1, Y_1 and Z_1 factors to $(k_1^2 + |q_1|^2 - K^2)^2 k_1^2$, and setting it to zero gives

$$|q_1|^2 = K^2 - k_1^2 \tag{49}$$

as expected for an evanescent wave with $q_1 = \mathrm{i}|q_1|$. From equations (48) and (49) we see that the x and z components of E_1 are related by

$$|q_1|Z_1 = \mathrm{i}KX_1\,. \tag{50}$$

The magnetic field in the cladding, from $\boldsymbol{B}_1 = \mu_1\boldsymbol{H}_1$ and (3), is given by

$$\boldsymbol{H}_1 = \frac{c}{\mathrm{i}\omega\mu_1}\nabla \times \boldsymbol{E}_1 = \frac{c}{\mathrm{i}\omega\mu_1}[|q_1|Y_1, -|q_1|X_1 - \mathrm{i}KZ_1, \mathrm{i}KY_1] \exp[\mathrm{i}Kx - |q_1|(z - d/2)]\,. \tag{51}$$

The even modes in the chiral slab are made up, as before, from a mix of positive and negative helicity eigenstates: from (9) and (13) we have

$$\boldsymbol{E}^{\mathrm{e}} = [q_+s_+ + Aq_-s_-, k_+c_+ - Ak_-c_-, \mathrm{i}K(c_+ + Ac_-)] \exp(\mathrm{i}Kx) \tag{52}$$

where $s_\pm = \sin(q_\pm z)$ and $c_\pm = \cos(q_\pm z)$ and $q_\pm^2 = k_\pm^2 - K^2$. The modes with E_y and E_z odd in z are

$$\boldsymbol{E}^{\mathrm{o}} = [q_+c_+ + Aq_-c_-, -k_+s_+ + Ak_-s_-, -\mathrm{i}K(s_+ + As_-)] \exp(\mathrm{i}Kx)\,. \tag{53}$$

From equations (3) and (4), the $\boldsymbol{H}$ field is determined in terms of $\boldsymbol{E}$:

$$\boldsymbol{H} = \frac{c}{\mathrm{i}\omega\mu}\nabla \times \boldsymbol{E} + \frac{\mathrm{i}\gamma}{\mu}\boldsymbol{E}\,. \tag{54}$$

The boundary conditions, namely continuity of the tangential components E_x, E_y, H_x and H_y of the electric and magnetic fields, give four relations at $z = d/2$ (a similar set obtained at $z = -d/2$ gives no new information, since even or odd symmetry has been assumed). After eliminating the unknown coefficients X_1, Y_1 and A from the four relations, we are left with the dispersion relation linking K to $k = n\omega/c$. For the even and odd modes, the dispersion relations are, respectively,

$$|q_1|(\epsilon\mu_1 + \epsilon_1\mu)\frac{\omega^2}{c^2}(T_+ + T_-) - 2k\left(k_1^2 T_+ T_- + |q_1|^2\right) = 0 \tag{55}$$

$$|q_1|(\epsilon\mu_1 + \epsilon_1\mu)\frac{\omega^2}{c^2}(C_+ + C_-) + 2k\left(k_1^2 C_+ C_- + |q_1|^2\right) = 0 \tag{56}$$

where

$$T_\pm = \frac{q_\pm}{k_\pm}\tan(q_\pm d/2) \qquad C_\pm = \frac{q_\pm}{k_\pm}\cot(q_\pm d/2)\,. \tag{57}$$

For comparison, the even and odd mode equations for the chiral slab between conducting plates, (25) and (27), can be written as

$$T_+ + T_- = 0 \qquad \text{and} \qquad C_+ + C_- = 0\,. \tag{58}$$

The equations (58) follow from (55) and (56) in the limit of perfectly conducting plates, for which ϵ_1 tends to minus infinity.

For an achiral waveguide ($\gamma \to 0$) we have $T_+ = T_-$ and the left-hand side of (55) factors to give

$$q\tan(qd/2) = |q_1|\mu/\mu_1 \qquad q\tan(qd/2) = |q_1|\epsilon/\epsilon_1 \tag{59}$$

which are the known dispersion relations for even TE and even TM modes, respectively. Likewise, $C_+ = C_-$ in the achiral limit, and the left-hand side of (56) factors to give the dispersion relations for odd TE and odd TM modes:

$$-q\cot(qd/2) = |q_1|\mu/\mu_1 \qquad -q\cot(qd/2) = |q_1|\epsilon/\epsilon_1\,. \tag{60}$$

When $\mu = \mu_1$ equations (55) and (56) reduce to those of [6], where dispersion relations are plotted for four values of G ranging from 0.001 to 0.05.

One difference between metallic and dielectric cladding for the chiral slab is in the cut-off frequencies: for metal plates the cut-off is independent of the chiral index γ for the constitutive relations (2) used here, with $k = n\omega/c$ having cut-off values $k_c = m\pi/d$ with integer m. In contrast, the dielectric cladding cut-offs, found from (55) and (56) by setting $|q_1|$ equal to zero, are given by

$$k_c^\pm = \frac{m\pi/d}{\sqrt{1 - n_1^2/n_\pm^2}} \tag{61}$$

($n_1^2 < n_\pm^2$ is assumed). The even modes have even m and the odd modes have odd m. For given m greater than zero, equation (61) gives two different frequencies at which propagation of guided waves begins.

The $m = 0$ mode bifurcates at zero frequency: in general, the dispersion relation (55) has two solutions beginning at $k = 0$, $K = 0$. To examine the behaviour near zero frequency, we set

$$K^2 = k^2[\alpha^2 + \beta^2(kd)^2 + \cdots] \tag{62}$$

and find that $\alpha = n_1/n$ (so that $K \to k_1$ and $|q_1|^2 = K^2 - k_1^2 \to 0$ at zero frequency), and that β satisfies a quadratic equation,

$$4(1-G^2)\beta^2 - 2\left(\frac{\epsilon_1}{\epsilon} + \frac{\mu_1}{\mu}\right)\left(1 - G^2 - \frac{n_1^2}{n^2}\right)\beta + \frac{n_1^2}{n^2}\left[(1+G)^2 - \frac{n_1^2}{n^2}\right]\left[(1-G)^2 - \frac{n_1^2}{n^2}\right] = 0\,. \tag{63}$$

When G is zero, the values of β satisfying (63) are

$$\beta_{\rm TE} = \frac{\mu_1}{2\mu}\left(1 - \frac{n_1^2}{n^2}\right) \qquad \beta_{\rm TM} = \frac{\epsilon_1}{2\epsilon}\left(1 - \frac{n_1^2}{n^2}\right) \tag{64}$$

which correspond, respectively, to the achiral TE and TM $m = 0$ modes, for which the dispersion relations were given in (59). The solutions of (63) are given by (64) plus terms of even order in the chirality parameter G; when $\mu = \mu_1$ the second-order terms simplify to

$$\Delta\beta_{\rm TE} = \frac{2(\epsilon_1/\epsilon)^2 G^2}{(1-\epsilon_1/\epsilon)^2} \qquad \Delta\beta_{\rm TM} = -\frac{(\epsilon_1/\epsilon)[1 + 3\epsilon_1/\epsilon - (\epsilon_1/\epsilon)^2 + (\epsilon_1/\epsilon)^3]G^2}{2(1-\epsilon_1/\epsilon)^2}\,. \tag{65}$$

Thus for small G the propagating modes are predominantly TE or TM. Note, however, the denominators $(1 - \epsilon_1/\epsilon)^2$: these are small when the dielectric constant of the cladding is close to that of the chiral slab. Thus index matching enhances the chirality effects, as has been noted in other circumstances [17].

As $|G|$ increases to the value $1 - (\epsilon_1\mu_1/\epsilon\mu)^{1/2} = 1 - n_1/n$, the TE or TM character is lost: the roots of (63) are now zero and

$$\frac{n - n_1}{2n - n_1}\left(\frac{\epsilon_1}{\epsilon} + \frac{\mu_1}{\mu}\right). \tag{66}$$

The form of (66) indicates an equal mix of TE and TM at $G = \pm(1 - n_1/n)$. At this value of $|G|$ either k_+ or k_- becomes equal to k_1: for example, if $G \to 1 - n_1/n$, $k_- = (1-G)k \to n_1 k/n = k_1$. In fact, we can see directly from (55) that when $G = 1 - n_1/n$, a formal solution valid for all K is $K = k_1$, because then q_1 and q_- are both zero. However, when q_1 is zero the fields in the cladding do not decrease with $|z|$, and so the $\beta = 0, q_1 = 0$ limit cannot be attained. An approach to this limit can be seen in the numerical explorations of [6]: see, in particular, their figure 3.

7. Discussion

We have presented analytic results for a chiral slab waveguide, bounded by either conducting plates, or by a dielectric cladding.

The conducting plate waveguide, which may find use at microwave frequencies, showed that propagating modes of different symmetry may cross. The phase speed ω/K is the same for both modes at the cross-over frequency, which was given by (46).

In the case of dielectric cladding, cross-over is also possible: for given $k = n\omega/c$ we look for solutions of (55) and (56) with common q_+ and q_-. Since

$$C_\pm = \left(\frac{q_\pm}{k_\pm}\right)^2 / T_\pm = \left(1 - \frac{K^2}{k_\pm^2}\right) / T_\pm \tag{67}$$

the cross-over condition arising from the simultaneous solution of (55) and (56) becomes a quadratic in T_+ (or in T_-). I have not been able to find a simple criterion for cross-over analogous to (46).

We have also calculated the low-frequency dispersion relation in the form (62), from which we can deduce the phase and group speeds of both of the modes in terms of the coefficient β given by the quadratic equation (63):

$$\begin{aligned} v_{\mathrm{p}} &= \frac{\omega}{K} = \frac{ck}{nK} = \frac{c}{n_1}\left[1 - \frac{1}{2}\left(\frac{n}{n_1}\right)^2 (\beta k d)^2 + \cdots\right] \\ v_{\mathrm{g}} &= \frac{\mathrm{d}\omega}{\mathrm{d}K} = \frac{c}{n}\frac{\mathrm{d}k}{\mathrm{d}K} = \frac{c}{n_1}\left[1 - \frac{3}{2}\left(\frac{n}{n_1}\right)^2 (\beta k d)^2 + \cdots\right]. \end{aligned} \tag{68}$$

An interesting situation arises when the chiral index γ is close to the difference between the average index of the chiral medium and the index of the cladding:

$$|\gamma| \to n - n_1 \qquad \text{or} \qquad |G| \to 1 - n_1/n\,. \tag{69}$$

In this special case, the analysis given in section 6 shows that for one of the even modes $\beta \to 0$, so dispersion tends to zero, both phase and group speeds tending to c/n_1. The limit of zero dispersion cannot be attained for the waveguide configuration discussed here, but zero dispersion is perhaps achievable for more complicated chiral waveguides.

In all cases the propagating modes have predominantly TE or TM character close to the cut-off frequency, provided the chirality is ‘small’. But in the dielectric-clad waveguide, we have seen that the chiral index γ is to be compared with the difference between the slab and cladding indices, $n - n_1$, which may itself be small. Thus chirality is enhanced by index matching, and numerically small chiral indices can be made to have a large effect.

Acknowledgment

This work has benefitted from reviewer comments and suggestions.

References

[1] Varadan V K, Lakhtakia A and Varadan V V 1988 Propagation in a parallel-plate waveguide wholly filled with a chiral medium *J. Wave–Material Interaction* **3** 267–72

[2] Eftimiu C and Pearson L W 1989 Guided electromagnetic waves in chiral media *Radio Sci.* **24** 351–9

[3] Chien M, Kim Y and Grebel H 1989 Mode conversion in optically active and isotropic waveguides *Opt. Lett.* **14** 826–8

[4] Pelet P and Engheta N 1990 Coupled-mode theory for chirowaveguides *J. Appl. Phys.* **67** 2742–5

[5] Cory H and Rosenhouse I 1991 Electromagnetic wave propagation along a chiral slab *IEE Proc.* H **138** 51–4

[6] Oksanen M, Koivisto P K and Lindell I V 1991 Dispersion curves and fields for a chiral slab waveguide *IEE Proc.* H **138** 327–34

[7] Mahmoud S F 1992 On mode bifurcation in chirowaveguides with perfect electric walls *J. Electromag. Waves Appl.* **6** 1381–92

[8] Paiva C R, Topa A L and Barbosa A M 1992 Semileaky waves in dielectric chirowaveguides *Opt. Lett.* **17** 1670–2

[9] Cory H and Gov S 1993 Mode energy transfer along a circular open chirowaveguide *Microwave Opt. Technol. Lett.* **6** 536–41

[10] Cory H 1993 Wave propagation along a closed rectangular chirowaveguide *Microwave Opt. Technol. Lett.* **6** 797–800

[11] Toscano A and Vegni L 1993 Effects of chirality admittance on the propagating modes in a parallel-plate waveguide partially filled with a chiral slab *Microwave Opt. Technol. Lett.* **6** 806–9

[12] Busse G and Jacob A F 1993 Complex modes in circular chirowaveguides *Electron. Lett.* **29** 711–3

[13] Qiu R C and Lu I-T 1994 Guided waves in chiral optical fibres *J. Opt. Soc. Am.* A **11** 3212–9

[14] Singh A K, Khastgir P and Singh O N 1995 Modal characteristics of EM wave propagation through a chirofibre with different core and cladding chiral admittances *Opt. Commun.* **115** 256–60
[15] Condon E U 1937 Theories of optical rotatory power *Rev. Mod. Phys.* **9** 432–57
[16] Silverman M P 1986 Reflection and refraction at the surface of a chiral medium: comparison of gyrotropic constitutive relations invariant or noninvariant under a duality transformation *J. Opt. Soc. Am.* A **3** 830–7
[17] Lekner J 1996 Optical properties of isotropic chiral media *Pure Appl. Opt.* **5** 417–43